

Detecting Nonclassical Correlations in Levitated Cavity Optomechanics

Andrey A. Rakhubovsky^{1,*}, Darren W. Moore^{1D},¹ Uroš Delić^{1D},^{2,3} Nikolai Kiesel,² Markus Aspelmeyer,^{2,3} and Radim Filip¹

¹*Department of Optics, Palacký University, 17. Listopadu 12, 771 46 Olomouc, Czech Republic*

²*Vienna Center for Quantum Science and Technology (VCQ), Faculty of Physics, University of Vienna, Boltzmanngasse 5, A-1090 Vienna, Austria*

³*Institute for Quantum Optics and Quantum Information (IQOQI), Boltzmanngasse 3, 1090 Vienna, Austria*



(Received 24 March 2020; revised 12 October 2020; accepted 28 October 2020; published 20 November 2020)

Nonclassical optomechanical correlations enable optical control of mechanical motion beyond the limitations of classical driving. Here we investigate the feasibility of using pulsed cavity optomechanics to create and verify nonclassical phase-sensitive correlations between light and the motion of a levitated nanoparticle in a realistic scenario. We show that optomechanical two-mode squeezing can persist even at the elevated temperatures of state-of-the-art experimental setups. We introduce a detection scheme based on optical homodyning that allows the revealing of nonclassical correlations without full optomechanical state tomography. We provide an analytical treatment using the rotating-wave approximation (RWA) in the resolved-sideband regime and prove its validity with a full numerical solution of the Lyapunov equation beyond the RWA. We build on parameters of current experiments for our analysis and conclude that the observation of nonclassical correlations, which are essential for quantum sensing, quantum engines, and quantum simulations with levitated nanoparticles, is possible with state-of-the-art capabilities. The general treatment can be applied to other optomechanical platforms.

DOI: 10.1103/PhysRevApplied.14.054052

I. INTRODUCTION

Nonclassical correlations between different quantum systems constitute the physical backbone of hybrid quantum devices. For example, electromagnetic radiation is used to connect atomic or solid-state quantum systems over long distances. In hybrid quantum systems, these interactions need to go beyond the limitations of classical interfaces. This can be verified by detecting nonclassical correlations, for example, using the Cauchy-Schwarz inequality for the second-order correlation function [1–4] or by direct observation of energy correlations [5–8]. These witnesses are phase insensitive. In contrast, phase-sensitive witnesses rely on the detection of quadrature correlations between homodyne detectors [9,10]. Revealing such correlations is a precursor for the evaluation of continuous-variable entanglement [11,12] that builds up in the interaction between quantum oscillators and light. Experimental demonstrations of entanglement, or two-mode squeezing, have been achieved between light and atoms [13–15] and between microwaves and mechanical motion [16,17]. In the optical domain, phase-insensitive detection of nonclassical correlations has been achieved in optomechanical photonic crystals [1,18,19].

The observation of nonclassical effects in cavity optomechanics is often inhibited by mechanical coupling to a thermal environment. It is therefore not surprising that most quantum optomechanics experiments to date are performed in a cryogenic environment. Several strategies have been proposed to circumvent the negative impact of the thermal environment [20,21]. One of the most promising approaches relies on utilizing pulsed cavity-optomechanical control [22], which was shown to be robust to the thermal noise of the mechanical environment and therefore does not rely on deep precooling of the mechanical motion [23]. In experimentally implementing such an approach, levitated cavity optomechanics [24–29] is particularly suitable due to its simple mechanical mode structure. Additionally, it provides an excellent isolation from the thermal environment [30,31]. With the recent demonstration of ground-state cooling in an optical cavity [29], the demonstration of nonclassical optomechanical correlations constitutes the next relevant step for levitated optomechanics. Accordingly, increasing theoretical effort devoted to obtaining nonclassical states [32] and correlations [33] with levitated nanoparticles is to be expected.

Here we demonstrate how phase-sensitive nonclassical correlations can be observed in a state-of-the-art optical levitation experiment at room temperature. We analyze the entanglement and generalized squeezing that is created

*rkhbvs@gmail.com

during a pulsed entanglement protocol with a moderate precooling (to an occupation of 10^4 phonons) and realistic heating rates. Our analysis builds on previous studies of the pulsed approach to optomechanical entanglement [16,22]. In contrast to these studies we also consider the nonadiabatic regime of a good cavity, in which the timescales of coupling and pulses exceed the cavity decay rate. Moreover, we propose a setting that allows direct verification of the nonclassical correlations by detecting the relevant quadratures in homodyne detection. Similar to the Duan-Giedke-Cirac-Zoller criterion [34], standardly employed in optomechanics [16,35,36], the proposed method gives a sufficient condition of nonclassical correlations. At the same time, our approach does not require full quantum state tomography of the optomechanical state and thus requires less experimental effort. We conclude that nonclassical correlations are observable in state-of-the-art levitated cavity optomechanics in a room-temperature environment without the need for precooling to the ground state. Our analysis is as well applicable to any optomechanical system capable of functioning in the linearized regime of the radiation-pressure coupling [37–41].

Creation and efficient verification of entanglement is crucial for a number of quantum technologies. Nonclassical correlations involving macroscopic objects enable entanglement-based quantum control schemes for such systems. This, in turn, helps to exploit their full potential for metrology and force, mass and acceleration sensing [42–55]. Another prospective field where nonclassical correlations can be applied is signal transduction and routing at the quantum level [56,57]. At the fundamental level nonclassical correlations with nanoparticles can be used for tests of quantum mechanics at macroscopic scales [58,59], testing of collapse models [60,61], or quantum thermodynamics [62]. An example of a possible application of nonclassical optomechanical correlations is the pulsed measurement-induced squeezers for mechanical states. Such squeezers have direct applications in nanomechanical engines [63–69] capable of reaching quantum limits of performance [66]. In the long run, methods for the efficient creation and verification of optomechanical entanglement find direct use in areas such as optomechanical arrays [70–72] where nonclassical correlations are useful for enhancing the coupling and extending it spatially.

II. RESULTS

A. Generation of the nonclassical correlations

In this manuscript we consider a pulsed optomechanical protocol to create nonclassical phase-sensitive correlations between a pulse of radiation and noisy mechanical oscillations of a levitated nanosphere. In levitated optomechanics, the radiation pressure enables a parametric interaction between the cavity light and oscillations of a nanoparticle

trapped inside the cavity in an externally applied Gaussian beam. The interaction can be enhanced and manipulated by a laser drive. Depending on the tuning of the drive, different types of optomechanical interaction can be observed. They can differ in their sensitivity to the noise of mechanical systems [73]. When the optomechanical system operates in the so-called resolved-sideband regime (when the cavity linewidth κ is smaller than the frequency of the mechanical motion of the particle Ω), in the particular case of resonant driving on the upper mechanical sideband, an effective amplifier-type interaction is established between the light and mechanics, with the two-mode squeezing (TMS) Hamiltonian expressed in terms of the ladder operators as $H_{\text{TMS}} = g(a_m a_L + \text{H.c.})$. This interaction is known to generate various forms of quantum correlations between the electric field of the light and the particle motion. In Ref. [16] this type of coupling was used to create electromechanical entanglement after precooling the mechanical oscillator from the initial occupation of approximately $n_0 = 40$ down close to the ground state. Advantageously, the highly mixed entanglement thus generated can be quite robust against the mechanical noise for a highly developed experimental platform [23] even without this precooling stage. This property is an important resource for transducers with hot mechanical systems [57,74–77]. Driving the system on the lower mechanical sideband enables parametric conversion between the light and mechanical motion with an effective beam-splitter (BS) Hamiltonian $H_{\text{BS}} = g(a_m a_L^\dagger + \text{H.c.})$. Using the toolbox of these interactions, it is possible to create and verify the nonclassical correlations in an optomechanical system.

The specific experimental setup we investigate is shown in Fig. 1 (see also Refs. [29,78]) with all the relevant parameters that are used throughout the paper summarized in Table I of Appendix A. An optical tweezer ($\lambda = 1064$ nm) traps a silica nanoparticle (radius $r \approx 70$ nm), providing an essentially harmonic trap with a radial frequency of $\Omega_m = 2\pi \times 190$ kHz. The nanoparticle is positioned at the axis of a high-Finesse cavity (cavity linewidth $\kappa \approx 2\pi \times 96.5$ kHz, length $l \approx 10$ mm) and at the intensity slope of the standing wave in an optically driven mode, resulting in the typical linearized optomechanical interaction ([30,79]). The particle is also interacting with a thermal environment given by the surrounding gas at a pressure of 10^{-6} mbar and room temperature, resulting in a dominant heating rate of 15 kHz. Recoil from scattered photons adds a smaller contribution of 6 kHz. Following the protocol of Ref. [22], nonclassical correlations are created by sending a blue-detuned light pulse (detuning $\Delta = \Omega_m$, duration $\tau = 6.6 \mu\text{s} = 8/\kappa$ coupling to mechanics $g = 2\pi \times 60$ kHz) onto the cavity. We assume the driving laser to be shot-noise limited. Laser phase noise manifests itself in an additional heating of the particle's motion at a moderate rate and is therefore covered in the following analysis. Precooling assumes only a moderate initial occupation of

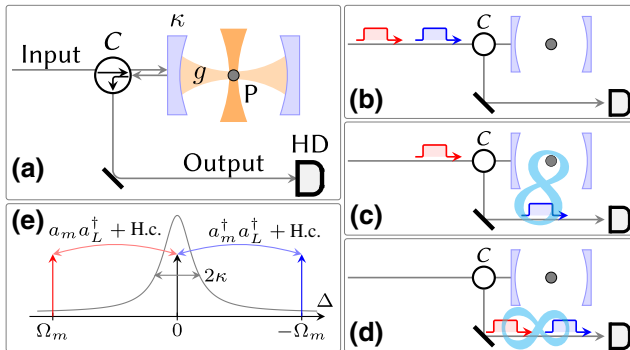


FIG. 1. A scheme of the pulsed protocol to generate and verify nonclassical correlations between the levitated nanoparticle and light. (a) A sketch of the proposed setup. A subwavelength particle (P), trapped within a single-mode cavity, is coupled to its mode via radiation pressure at rate g . (b)–(d) Two light pulses, blue and red detuned enter the cavity to interact with the particle and are subsequently routed to the homodyne detector (HD) via the circulator (C). The cyan eightlike symbol denotes non-classical correlations between different parts of the system. (e) Depending on the detuning $\Delta = \omega_{\text{cav}} - \omega_p$ of the pump, different types of interaction take place between the center-of-mass motion of the particle and the intracavity field.

$n_0 \leq 10^4$ phonons, because no significant improvement of entanglement is achieved by lower initial occupations. In Sec. II A we analyze these optical-mechanical correlations in detail. To detect the correlations a second, red-detuned readout pulse is used (detuning $\Delta = -\Omega_m$, coupling g and duration τ equal for both pulses). We analyze the non-classical correlations observed between these pulses in homodyne detection after emission from the optical cavity in Sec. II B. Losses of the cavity mirrors provide the dominant limitation on efficiency. In our results we use current [78] and realistic (e.g., Ref. [80]) detection efficiencies of 0.4 and 0.8, respectively.

We propose to utilize this interaction of the center-of-mass displacement of a levitated nanoparticle with a pulse of light impinging upon the cavity to prepare a nonclassical correlation between the leaking light and noisy mechanical motion. In the presence of the pump, the annihilation operators of the optical (B) and the mechanical (a_m) modes transform according to the set of linear input-output

TABLE I. Parameters of the experimental setup [29,78] used for simulations.

Parameter	Experimental run	Dimensionless unit	Simulations
κ (kHz)	$2\pi \times 96.5$	1	1
g (kHz)	$2\pi \times 60$	0.62	≤ 0.6
Ω_m (kHz)	$2\pi \times 190$	1.96	2
Γ_{gas} (kHz)	$2\pi \times 15$	0.16	0.16
Γ_r (kHz)	$2\pi \times 6$	0.06	0.06

relations

$$B^{\text{out}} = \sqrt{\mathcal{G}} B^{\text{in}} + \sqrt{\mathcal{G} - 1} a_m^\dagger(0), \quad (1a)$$

$$a_m(\tau) = \sqrt{\mathcal{G}} a_m(0) + \sqrt{\mathcal{G} - 1} B^{\text{in},\dagger}, \quad (1b)$$

which corresponds to a two-mode squeezing interaction with the gain $\mathcal{G} \approx \exp[2g^2\tau/\kappa]$ determined by the values of the optomechanical coupling rate g , cavity linewidth κ , and the interaction duration τ . It is important to stress that B^{out} describes a certain mode of light defined by a particular temporal profile (see Appendix B 1 for details).

It is known that the unitary two-mode squeezing interaction can entangle the participating modes even in the case of large initial noise in one of the modes [73]. The optomechanical cavity, however, is open and therefore its dynamics is not simply unitary. The cavity is coupled to the detection channel and therefore has a finite linewidth κ . The collection efficiency is nonunity, so a part of the signal from the optomechanical cavity is lost. This effect is easy to describe as pure loss before the detection. The nanoparticle experiences heating at a rate Γ due to a number of factors, of which the two most important are collisions with the residual gas inside the vacuum chamber and the recoil heating. Our task is therefore to analyze the robustness of the protocol to these imperfections and determine to what extent the performance of a realistic levitated system can approach the idealised unitary two-mode squeezing. The analysis of the operation of a levitated system has a few peculiarities compared to conventional bulk devices. Levitated systems are capable of demonstrating rather strong optomechanical coupling comparable to the cavity linewidth $g \sim \kappa$. This allows operation beyond the adiabatic regime (in which the intracavity light mode is unpopulated). This, in turn, requires a precise definition of the temporal modes for the homodyne detection. Another peculiarity is a rather stringent limit on the duration of operation τ set by the inverse heating rate: $\Gamma\tau \leq 1$.

To visualize the nonclassical correlations in the system formed by the leaking pulse and the mechanical oscillator, we use entanglement evaluated in terms of logarithmic negativity [11] and the two-mode squeezing. The latter has the meaning of the maximal amount of squeezing that can be directly extracted from the system by a global Gaussian passive transformation [12]. Both quantities can be straightforwardly computed for a bipartite Gaussian quantum state. We evaluate the nonclassicality as a function of the heating rate in Fig. 2(a). It can be seen that the heating influences the correlations only beyond a certain point (in Fig. 2, approximately 10^{-2}), after which the nonclassicality decreases from the value $E_N \approx 1.7$ and eventually vanishes after a certain value Γ_{crit} . In Fig. 2 two values of the heating rate are emphasized: Γ_{gas} set by the collisions with the residual gas in the trapping chamber and

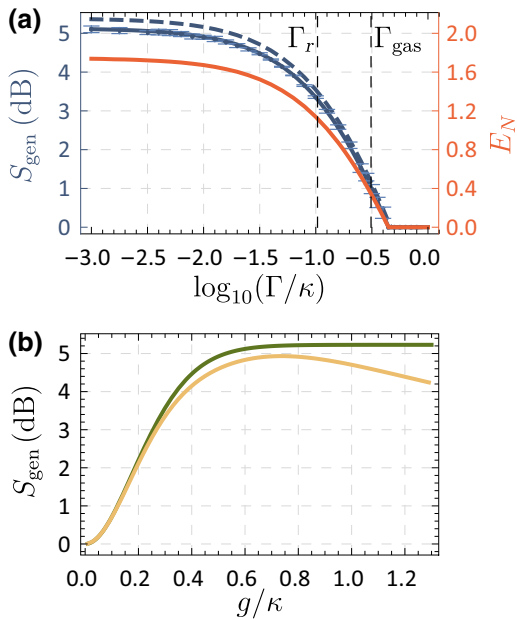


FIG. 2. (a) Robustness of the nonclassicality of the correlations between light and mechanical motion of the levitating nanoparticle [see Fig. 1 (c)]. Two-mode squeezing S_{gen} (dark blue) and logarithmic negativity E_N (light red) as functions of the heating rate Γ (logarithmic scale, in units of κ) assuming an initial mechanical occupation of $n_0 = 10^4$. The dashed line shows the two-mode squeezing computed without the rotating-wave approximation. The error bars on the blue curve are obtained from the numerical simulation (see the text). (b) Two-mode squeezing as a function of the coupling rate. The dark green line shows the adiabatic regime; light yellow, full solution. The two solutions coincide well at values corresponding to the weak coupling where the adiabatic approximation is valid. Numerical parameters are $g = 0.6\kappa$, $\tau = 8/\kappa$, $\Omega = 2\kappa$.

the recoil heating [81], and Γ_r , set by the recoil heating alone. The latter is determined by the properties of the particle and the trap, and appears to be a fundamental limitation for a given experimental environment. We, however, see that this limitation is not prohibitive for the feasible setup.

The behavior of the nonclassical correlations as a function of the heating rate depends on the particular regime of operation determined by the coupling rate g and the pulse duration τ . For Fig. 2 we numerically optimized the two-mode squeezing as a function of g , τ to persist at as high Γ as possible while providing at least 1 dB of squeezing at $\Gamma = \Gamma_{\text{gas}}$. One regime of interest is the so-called *adiabatic* regime, in which the cavity mode is eliminated and the interaction approaches the ideal unitary form (1) of the pure two-mode squeezing. If the cavity linewidth κ is the dominant rate of the system, the cavity excitations instantaneously leak. Thereby, the propagating light is virtually directly coupled to the mechanical motion, which allows transformations of the form (1). In the adiabatic

regime (see Appendix D) the magnitude of the squeezing is determined by the interaction gain $\mathcal{G} = \exp[2g^2\tau/\kappa]$ and the influence of the thermal noise from the mechanical environment is set by the product $\Gamma\tau$.

The formal requirements of the adiabatic regime can be cast as $\kappa \geq g, \tau^{-1}, \Gamma$ therefore the regime needs the pulses to be rather long with $\kappa\tau \gg 1$. The available duration of the pulse, however, is limited from above by the heating rate. Indeed, the decoherence caused by interaction with the environment is manifested in the form of an admixture of thermal noise to the quantum state of the particle with the variance of the thermal noise proportional to $\Gamma\tau$. When the condition $\Gamma\tau \ll 1$ is met, the environment has virtually no impact on the nonclassicality, which can be seen from Fig. 2(a). This, however, with the currently observable heating rates, sets an upper limit on allowed pulse durations τ . This, in turn, makes the adiabatic regime infeasible, and makes the full dynamics richer than just unitary two-mode squeezing. We, however, see from Fig. 2(b) that, for weak coupling rates $g \ll \kappa$ that satisfy the adiabatic requirements, the performance of the full solution can be approximated by the adiabatic one. Creation of strong nonclassical correlations, however, requires an excursion outside of the adiabatic regime.

To produce the curves, we also assume that both subsystems experience a loss characterized by transmittance $\eta = 0.8$ ($\eta = 1$ corresponding to the lossless case). For the optical mode, this loss describes different possible imperfections including nonperfect detection and collection efficiency, and also imperfect temporal and spatial mode overlap. For the mechanics, the loss simulates a process of transferring the mechanical state to a measurable system, as the mechanical state itself is not accessible. In particular, a readout of the mechanical oscillator's state done by a red-detuned pulse is also equivalent to an almost noiseless lossy map to light [82,83], so the lossy model gives a good grasp of this process. The proper simulation of the readout of the mechanical state by a red-detuned pulse is given in Sec. II B. Importantly, the figure shows that the nonclassical correlations of interest are quite robust to pure loss. The correlations are also created regardless of the initial temperature of the mechanics. Figure 2(a) is plotted for a realistic value of initial occupation of $n_0 = 10^4$, and decreasing the occupation further does not increase magnitudes of either the two-mode squeezing or the logarithmic negativity.

The error bars in Fig. 2(a) are obtained from numerical simulation. A covariance matrix of the final bipartite state depends on a number of parameters, including the coupling rate g , interaction duration τ , the initial occupation n_0 , and the reheating rate Γ . For a certain value of the latter, we take an ensemble of 40 numerical samples of covariance matrices assuming that each of the other parameters ϵ (with ϵ being one of g , τ , or $\log_{10} n_0$) is uniformly distributed within the region $0.9\epsilon \leq \epsilon \leq 1.1\epsilon$.

To perform a complete check of the robustness of our proposed setup, we also compute the two-mode squeezing beyond the rotating-wave approximation (RWA) by numerically solving the Lyapunov equation for the covariance matrix (see Appendix B3). The RWA significantly simplifies the solution, as it allows us to omit the terms in the interaction that oscillate with periods proportional to 2Ω , which are off resonant for $\Omega \gg \kappa, g$. The accuracy of the RWA thereby increases when Ω becomes large compared to the other frequencies of the system. The solution beyond the RWA includes the omitted terms that represent the beamsplitter-type interaction between light and mechanics. Our analysis [Fig. 2(a), dashed line] shows that, for a moderate sideband resolution ($\Omega = 2\kappa$), inclusion of these terms slightly improves the creation of non-classical correlations thanks to additional cooling of the nanoparticle. As Ω increases, the dashed line approaches the solid line until at approximately $\Omega = 10\kappa$ there is no difference caused by inclusion of the beyond-RWA terms. For details, see Appendix B3.

B. Detection of the correlations via homodyne measurement

In this section we provide a recipe to experimentally assess the nonclassical correlations between the light and mechanics created by the blue-detuned pulse. The quantum correlations can be detected by swapping the mechanical state to the leaking pulse followed by a tomography of the quantum state of the two pulses. Using homodyne detection, we can reconstruct the full covariance matrix from which it is possible to evaluate an arbitrary measure of non-classicality, in particular, the two-mode squeezing and the entanglement. We can also design an experimentally less resource-demanding two-mode squeezing witness that can show the presence of entanglement requiring fewer experimental runs. In particular, we note that the optomechanical entanglement manifests itself in the form of two-mode squeezing that is a squeezing of a weighted combination of quadratures of light and mechanics. The combination quantitatively coincides with that provided by the theory of the unitary two-mode squeezing in the adiabatic regime.

Our proposal of the evaluation of the correlations created by the blue-detuned pules relies on use of a subsequent pulse tuned to the lower mechanical sideband of the cavity. In such a case, depending on the parameters, the interaction between the light and the nanoparticle's motion approaches the unitary beamsplitter-type coupling. The input-output relations for this coupling, similarly to Eq. (1), can be cast in the form

$$\mathbf{R}^{\text{out}} = \sqrt{\mathcal{T}} \mathbf{R}^{\text{in}} + \sqrt{\mathcal{T} - 1} a_m(\tau_i), \quad (2a)$$

$$a_m(\tau_f) = \sqrt{\mathcal{T}} a_m(\tau_i) + \sqrt{\mathcal{T} - 1} \mathbf{R}^{\text{in}}, \quad (2b)$$

where $\tau_i = \tau + \tau_D$ is the instant at which the state swap starts; this instant incorporates some delay τ_D after the entangling interaction has ended, and $\tau_f = \tau_i + \tau_R$ is the instant at which the state swap is completed. The transmittance \mathcal{T} is determined by the strength of the pump and the duration of the swap τ_R . It is easy to show (see Appendix B) that $a_m(\tau_i)$ is equivalent to $a_m(\tau)$ entering Eq. (1) up to some thermal noise defined by the duration of the delay τ_D . The correlations between the quadratures of the modes defined by annihilation operators \mathbf{B}^{out} and \mathbf{R}^{out} will then reveal the original correlations between \mathbf{B}^{out} and $a_m(\tau)$ created by the blue-detuned pulse.

Using the standard approach outlined in Appendix B, we can evaluate the nonclassical correlations that persist in the bipartite system formed by the two pulses. Figure 3, where we plot the two-mode squeezing as a function of the heating rate of mechanics, shows the robustness of the correlations to the mechanical decoherence. It can be seen that compared to the purely unitary description of Eq. (2) the readout is not purely lossy, but in fact adds noise. The noise, however, is moderate so it does not prohibit creation

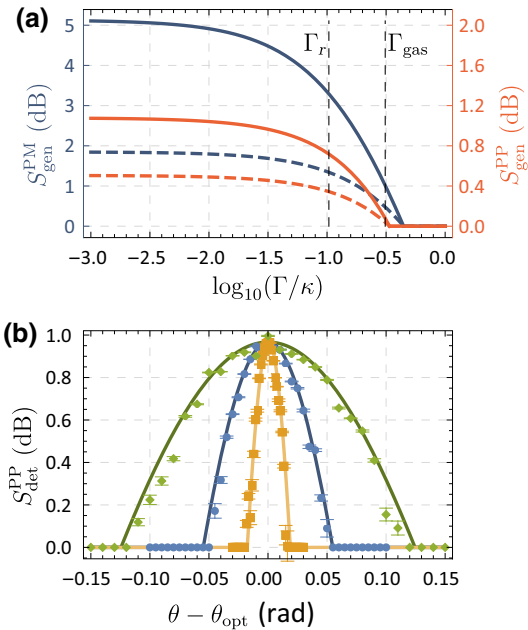


FIG. 3. Detection of nonclassical correlations with homodyne measurement on leaking light. (a) Comparison of the two-mode squeezing of the leaking entangling pulse and mechanical motion [S^{PM} ; dark blue; Fig. 1(c)] and two-mode squeezing of two pulses [S^{PP} , light red; Fig. 1(d)] as a function of the heating rate. Full and dashed lines show cases of detection efficiency $\eta = 0.8$ and $\eta = 0.4$, respectively. (b) Detectable two-mode squeezing $-10 \log_{10} \text{Var}X_{\text{gen}}[\phi^{\text{opt}}, \theta_B, \theta_R^{\text{opt}}]$ as a function of the homodyne angle θ_B for two other angles set to their optimal values. Heating rate $\Gamma = 0.1\kappa$. Different colors show the initial occupation of mechanics (from wider to narrower curve) $n_0 = 1$ for dark green, $n_0 = 10$ for blue, and $n_0 = 100$ for light yellow. Error bars are obtained by numerical simulations.

of correlations between the two pulses with experimentally feasible parameters. The graphs are obtained for the parameters optimized to make the correlations observable at as high heating rates Γ as possible. From the figure we conclude that with a feasible heating rate and detection efficiency one can observe the two-mode squeezing in a state-of-the-art experiment. The correlations between the two pulses are similarly robust to the initial mechanical occupation just as were the correlations between the mechanics and the entangling pulse.

A full tomography of the bipartite Gaussian state of the two pulses requires estimation of all ten independent entries of their covariance matrix. Instead, to reduce the experimental cost of the detection, we propose to use the fact that the two-mode squeezing manifests itself in the form of suppression of one of the eigenvalues of the covariance matrix (CM) below the level of the shot noise. This means that in the optimal basis, in which the CM is brought to the diagonal form, the smallest eigenvalue enters the CM as a variance of one of the quadratures. Therefore, by adjusting the homodyne detection, it is possible to perform the measurement in this particular basis and to obtain the smallest eigenvalue directly.

To demonstrate the possibility of the two-mode squeezing observation, we analyze a generalized quadrature of the bipartite system, defined as

$$X_{\text{gen}}[\phi, \theta_B, \theta_R] = X_B^{\theta_B} \cos \phi + X_R^{\theta_R} \sin \phi, \quad (3)$$

where we define the quadratures of individual subsystems in the bases rotated by an angle θ : $X_i^\theta := X_i \cos \theta + P_i \sin \theta$. A certain choice of ϕ defines the weight with which quadratures of each of the systems enter the generalized quadrature. In a particular experimental run, the values of angles θ are defined by the phase of the local oscillator of the homodyne detector. The angle ϕ can be adjusted in postprocessing of the measurement results. Transformation to the generalized quadrature (3) represents the most general passive Gaussian bipartite transformation possible. To rule out the product states where one mode is squeezed, we consider only the bipartite states where each of the quadratures $X_{B,R}$ has a variance above the shot-noise level (which is the case occurring in the optomechanical two-mode squeezing), while their combination exhibits squeezing.

The variance of $X_{\text{gen}}[\phi^{\text{opt}}, \theta_B, \theta_R^{\text{opt}}]$ computed for our system is presented at Fig. 3(b). We observe that, for certain values of ϕ^{opt} and θ , the generalized quadrature is squeezed below the shot-noise level. Both curves have the same magnitude, which shows the insensitivity of the correlations to the initial occupation n_0 ; however, a lower occupation simplifies the detection via homodyne since the squeezing can be seen in a wider range of the homodyne angle θ . In other words, cooling closer to the ground state allows an order of magnitude less precise adjustment of

the homodyne angles. This is advantageous, since in an experiment the homodyne angles $\theta_{B,R}$ have to be set in advance to the values that have to be estimated from the theory. Such an estimation relies on the calibration of the system parameters and can be error prone. Increasing the initial occupation also increases the demand for the precision with which the homodyne angle has to be determined. Simple calculations (see Appendix D) yield an estimate $\theta_{\text{max}} \propto 1/\sqrt{n_0}$ for the maximal imprecision after which the squeezing vanishes. Note that, for occupations up to as high as $n_0 \approx 10^4$, the required precision $\delta\theta$ does not exceed the value $\theta_{pn} = 1.7$ mrad attained in Ref. [84].

In order to verify the robustness of this detection scheme against the fluctuations of the system parameters, we simulate such fluctuations numerically. For each value of the deviation from the optimal homodyne angles $\delta\theta$, we compute the mean and the variance of squeezing for an ensemble of 20 realisations assuming each of the parameters ϵ (initial occupation n_0 , coupling rates g_k and durations τ_k of both pulses, and the heating rate Γ) is randomly uniformly distributed within the range $0.9 \leq \epsilon \leq 1.1$ of the equilibrium value. The homodyne angles $\theta_{B,R}$ assume the same values across the realisations to simulate a situation where they are set prior to the experiment. In contrast, the optimal superposition angle ϕ is determined for each realisation individually, because the optimisation with respect to this angle is possible in postprocessing. The result of this simulation determines the error bars in Fig. 3(b). The graph shows that the fluctuations of the parameters do not influence the detection much.

III. CONCLUSIONS

In this manuscript we demonstrate the capability of linearized Gaussian dynamics of a levitated optomechanical system (a levitated particle inside an optical cavity) to create nonclassical correlations persisting at high initial temperatures of the mechanical mode. Using the formalism of Heisenberg-Langevin equations and input-output theory, we search for two-mode squeezing and entanglement (the logarithmic negativity). While heating of the particle by the environment is the main limiting factor, we find that nonclassical correlations can persist at parameters of current experiments. These correlations are robust against experimental imperfections such as losses or heating effects, and can be efficiently detected by homodyning the cavity output field. This is achieved by a readout pulse that maps the correlations to a two-mode squeezed optical system.

The creation and observation of the described nonclassical correlations is a powerful resource for quantum controlling levitated nanoparticles without the need to initialize the mechanical system in the quantum ground state. Future experiments may well combine such correlation-based control with the additional capability of spatiotemporal

driving of the optical potential landscape beyond quadratic potentials [85] or non-Gaussian detection [19,33]. These complementary methods can provide a rich toolbox for optimal non-Gaussian quantum state control.

ACKNOWLEDGMENTS

A.A.R., D.M., and R.F. are supported by the Czech Scientific Foundation (project 20-16577S), the MEYS of the Czech Republic (Grants No. 731473 and No. 02.1.01/0.0/0.0/16_026/0008460), and the Czech Ministry of Education (project LTC17086 of the INTER-EXCELLENCE program), and have received national funding from the MEYS and funding from the European Union's Horizon 2020 (2014–2020) research and innovation framework programme under Grant No. 731473 (project 8C18003 TheBlinQC). Project TheBlinQC received funding from the QuantERA ERA-NET Cofund in Quantum Technologies implemented within the European Union's Horizon 2020 Programme. U.D., N.K., and M.A. acknowledge support from the European Research Council (ERC CoG QLev4G), TheBlinQC (Project No. 864032; via the EC, the Austrian ministries BMDW, and BMBWF and research promotion agency FFG), the Austrian Science Fund (FWF) START programme (Y 952-N36), the doctoral school CoQuS (Project W1210), and the Austrian Marshall Plan Foundation.

APPENDIX A: PARAMETERS USED FOR SIMULATIONS

The experimental parameters listed in Table I are as reported in Refs. [29,78]. The reported experimental values are converted to dimensionless units where $\kappa = 1$ (third column). The fourth column lists the values of the parameters used for the simulations to create Figs. 2 and 3.

APPENDIX B: ESTIMATING COVARIANCE MATRICES

1. Hamiltonian formulation

In this manuscript we consider a levitated optomechanical system as depicted in Fig. 1. At the heart of the scheme is the levitated subwavelength dielectric particle trapped in a high vacuum within a high- Q optical cavity assumed to be a single-mode cavity described by canonical quadratures X_c , P_c , with eigenfrequency ω_{cav} and linewidth κ . Within the cavity, the subwavelength particle is held in a harmonic trap so that the particle's center-of-mass motion can be modeled as a harmonic oscillator with quadratures X_m , P_m of eigenfrequency Ω . We normalize the quadratures such that $[X_k, P_k] = 2i$, with $k = c, m$. The two modes interact via radiation pressure by a linear coupling at rate g . In the presence of a strong classical pump at ω_p the Hamiltonian of the system is linearized and in the

frame rotating at $\omega_p a^\dagger a$ (see Refs. [86–88]) reads

$$H = \Delta(X_c^2 + P_c^2)/4 + \Omega(X_m^2 + P_m^2)/4 - gX_c X_m, \quad (\text{B1})$$

where $\Delta = \omega_{\text{cav}} - \omega_p$ is the detuning of the pump and $g = (\partial\omega_{\text{cav}}/\partial X_m)\sqrt{\langle n_p \rangle}$ is the optomechanical coupling rate enhanced by $\langle n_p \rangle$, the mean number of intracavity photons due to the pump.

It is illustrative to rewrite the Hamiltonian (B1) in the rotating frame defined by the first two terms of H . In this frame, only the interaction term remains. Introducing the annihilation operators for both mechanics and the cavity mode as $a_k = (X_k + iP_k)/2$, the interaction Hamiltonian can be written as

$$-H/g = a_c a_m e^{-i(\Omega+\Delta)t} + a_c^\dagger a_m e^{-i(\Omega-\Delta)t} + \text{H.c.} \quad (\text{B2})$$

The Hamiltonian has the form of a sum of a beamsplitter-type term and a two-mode-squeezing term, both modulated by an exponential. In the important cases of the resonantly detuned pump with $\Delta = \pm\Omega$, one of the terms in the interaction becomes resonant, and the other, on the contrary, off resonant. In particular, if the drive is detuned to the higher mechanical sideband, $\Delta = -\Omega$, the interaction reads

$$H = -ga_c a_m - ga_m a_c^\dagger e^{-2i\Omega t} + \text{H.c.} \quad (\text{B3})$$

If the condition of *resolved sideband*, $\Omega \gg \kappa$, holds, as it is in a significant fraction of the contemporary optomechanical experiments, the second term is indeed far from the cavity resonance, and is resonantly suppressed. Therefore, the interaction Hamiltonian approaches the two-mode-squeezing form. A similar reasoning can be applied to show that, when $\Delta = \Omega$, the interaction takes the form of a beamsplitter-type coupling with Hamiltonian $H \propto a_m a_c^\dagger$.

In the general case, taking into account damping and dissipation starting with the Hamiltonian (B1), we can write the system of Heisenberg-Langevin equations in the vector form

$$\dot{\mathbf{u}} = \mathbb{A} \cdot \mathbf{u} + \mathbf{n}, \quad (\text{B4})$$

where $\mathbf{u} = (X_c, P_c, X_m, P_m)$ is the vector of unknowns and $\mathbf{n} = (\sqrt{2\kappa}X^{\text{in}}, \sqrt{2\kappa}Y^{\text{in}}, 0, \sqrt{2\gamma}\xi^{\text{th}})$ is the vector of input fluctuations. We assume the optical input field to be in vacuum. The mechanical fluctuations ξ^{th} stem from different sources including collisions with the residual gas particles and recoil heating. We assume for ξ^{th} Markovian Gaussian statistics and describe it by a thermal state with mean occupation n_{th} ; γ is the viscous damping rate. The two parameters are conveniently combined in the experimentally detectable reheating rate $\Gamma \equiv \gamma n_{\text{th}}$. To summarize, the noises obey the statistics [with the notation for the

Jordan product $\langle \mathbf{a} \circ \mathbf{b} \rangle_{ij} \equiv \frac{1}{2}(\langle \mathbf{a}_i \mathbf{b}_j + \mathbf{b}_j \mathbf{a}_i \rangle)$:

$$\langle \xi^{\text{th}}(t) \circ \xi^{\text{th}}(t') \rangle = (2n_{\text{th}} + 1)\delta(t - t'), \quad (\text{B5})$$

$$\langle Q^{\text{in}}(t) \circ Q^{\text{in}}(t') \rangle = \delta(t - t') \quad \text{with } Q = X, Y. \quad (\text{B6})$$

The drift matrix \mathbb{A} has the form

$$\mathbb{A} = \begin{pmatrix} -\kappa & -\Delta & 0 & 0 \\ \Delta & -\kappa & 2g & 0 \\ 0 & 0 & 0 & \Omega \\ 2g & 0 & -\Omega & -\gamma \end{pmatrix}. \quad (\text{B7})$$

Equation (B4) has the solution

$$\mathbf{u}(t) = \mathbb{M}(t) \cdot \mathbf{u}(0) + \int_0^t ds \mathbb{M}(t-s) \cdot \mathbf{n}(s), \quad (\text{B8})$$

where $\mathbb{M}(t) \equiv \exp[\mathbb{A}t]$. The solution is valid for a time-independent matrix \mathbb{A} .

One can write the solution for the light leaking from the cavity using input-output relations

$$\mathbf{u}^{\text{out}} = -\frac{1}{\sqrt{2\kappa}} \tilde{\mathbf{n}} + \sqrt{2\kappa} \tilde{\mathbf{u}}, \quad (\text{B9})$$

where the tilde means taking the first two elements of a vector, e.g., $\tilde{\mathbf{u}} = (X_c, P_c)$. The leaking field $\mathbf{u}^{\text{out}}(t) = [X^{\text{out}}(t), Y^{\text{out}}(t)]$ describes a continuum of modes of semi-infinite space. Of those we are interested in the one mode that is being detected in the homodyne detector. The quantum state of the leaking pulse is therefore described by the canonical quadratures of that mode defined as

$$\vec{U} \equiv (X^{\text{out}}, Y^{\text{out}}) = \int_0^\tau ds \mathbf{u}^{\text{out}}(s) f^{\text{out}}(s), \quad (\text{B10})$$

where the function f^{out} defines the temporal profile of the mode to be measured. In order to fully capture the necessary information it is important to tailor a specific profile. This is particularly evident for the readout (red) pulse that necessarily needs to be adjusted to retrieve the state of mechanics at the beginning of this pulse since the initial mechanical state couples to a particular temporal mode. For both pulses, we use the profiles equal to the element of the matrix \mathbb{M} that corresponds to the transfer of the initial mechanical quadratures to the light. In particular, for the readout pulse, we choose $f^{\text{out}}(t) \propto \mathbb{M}_{13}(t)$. Optimization of the profiles might be beneficial for the observation of stronger nonclassical correlation, though such observation is beyond the scope of the present work. In an experiment, different profiles f^{out} can be used by means of frequent sampling of the leaking signal and assembling a weighted

sum of the samples in postprocessing [89,90]. State-of-the-art detectors allow detection at rates that significantly exceed the characteristic rates of the levitated optomechanical systems; therefore, there is a certain freedom in selecting f^{out} .

2. Rotating-wave approximation

In a typical optomechanical system, particularly in the levitated optomechanics, the optomechanical coupling rate is smaller than the cavity linewidth: $g \ll \kappa$. Combined with the condition of the resolved sideband $\kappa \ll \Omega$ this suggests that creation of the optomechanical correlations happens at the timescale slower than the oscillations at Ω . This justifies a transition to the rotating frame, defined by the first two terms of Eq. (B1), $H_{\text{rf}} = \Delta(X_c^2 + P_c^2)/4 + \Omega(X_m^2 + P_m^2)/4$, with a subsequent application of the RWA.

The transition to the rotating frame amounts to the transformation from the vector \mathbf{u} to the vector of the quadrature amplitudes $\mathbf{u} = \mathbb{R} \cdot \mathbf{v}$, where $\mathbb{R} = \mathbb{R}_2(\Delta t) \oplus \mathbb{R}_2(\Omega t)$ and

$$\mathbb{R}_2(\alpha) = \begin{pmatrix} \cos \alpha & \sin \alpha \\ -\sin \alpha & \cos \alpha \end{pmatrix}. \quad (\text{B11})$$

The new vector of unknowns contains the quadrature amplitudes $\mathbf{v} = (X_c^{(c)}, X_c^{(s)}, X_m^{(c)}, X_m^{(s)})$ that on the timescale of mechanical frequency do not change significantly. The quadrature amplitudes obey a vector equation

$$\dot{\mathbf{v}} = \mathbb{A}^{(v)} \cdot \mathbf{v} + \mathbf{n}^{(v)}, \quad (\text{B12})$$

where

$$\mathbb{A}^{(v)} = \mathbb{R}^{-1} \cdot (\mathbb{A}\mathbb{R} - \dot{\mathbb{R}}), \quad \mathbf{n}^{(v)} = \mathbb{R}^{-1} \cdot \mathbf{n}. \quad (\text{B13})$$

The matrix $\mathbb{A}^{(v)}$ defined in this fashion contains terms that are rapidly oscillating compared to the rates g, κ, γ . The RWA amounts in dropping these terms. As a result, we obtain

$$\mathbb{A}_v|_{\text{RWA}} = \begin{pmatrix} -\kappa & 0 & 0 & g_r - g_b \\ 0 & -\kappa & g_r + g_b & 0 \\ 0 & g_r - g_b & -\frac{\gamma}{2} & 0 \\ g_r + g_b & 0 & 0 & -\frac{\gamma}{2} \end{pmatrix}. \quad (\text{B14})$$

Here g_r and g_b are the optomechanical coupling rates enabled by pumping on the correspondingly lower and upper mechanical sidebands of the cavity. We assume that during the entangling (blue detuned, $\Delta = -\Omega$) pulse, $g_b = g$, $g_r = 0$. In a similar fashion, during the readout pulse (red detuned, $\Delta = \Omega$), we set $g_b = 0$, $g_r = g$. Between the pulses, there is no optomechanical interaction,

so the two modes (optical and mechanical) only experience decay and decoherence. The statistics of $\mathbf{n}^{(v)}$ take the following simple form in the RWA:

$$\langle \mathbf{n}^{(v)}(t) \circ \mathbf{n}^{(v)}(t') \rangle = \text{diag}[2\kappa, 2\kappa, 2\Gamma, 2\Gamma] \delta(t - t'). \quad (\text{B15})$$

In the RWA then Eq. (B12) is a system of linear differential equations that can be solved in a manner similar to Eq. (B8). With help of Eqs. (B9) and (B10) where again $f^{\text{out}}(t) \propto \mathbb{M}_{13}(t)$ we can write a solution for the necessary covariance matrix.

3. Lyapunov equation

One way to investigate the Gaussian dynamics described by Eq. (B12) is to use the Lyapunov equation. For the covariance matrix \mathbb{V} corresponding to the vector \mathbf{v} , it reads

$$\dot{\mathbb{V}} = \mathbb{A}^{(v)} \cdot \mathbb{V} + \mathbb{V} \cdot (\mathbb{A}^{(v)})^\top + \mathbb{D}^{(v)}, \quad (\text{B16})$$

where we keep the terms oscillating at 2Ω in $\mathbb{A}^{(v)}$, and $\mathbb{D}^{(v)}$ is the diffusion matrix containing correlations of the noises

$$\langle \mathbf{n}^{(v)}(t) \circ \mathbf{n}^{(v)}(t') \rangle = \mathbb{D}^{(v)} \delta(t - t'); \quad (\text{B17})$$

beyond the RWA it reads

$$\mathbb{D}^{(v)} = \begin{pmatrix} 2\kappa & 0 & 0 & 0 \\ 0 & 2\kappa & 0 & 0 \\ 0 & 0 & 2\Gamma[1 + \cos(2\Omega t)] & 2\Gamma \sin(2\Omega t) \\ 0 & 0 & 2\Gamma \sin(2\Omega t) & 2\Gamma \sin[1 + \cos(2\Omega t)] \end{pmatrix}. \quad (\text{B18})$$

We are, however, interested in the solution for the pulses of the leaking light. Taking a derivative of Eq. (B10) over time, we can obtain equations of motion for the pulse quadratures. Then we can write, for a six vector $\mathbf{w} = ([\mathbf{v}]_{1 \times 4}, \mathbf{X}^{\text{out}}, \mathbf{Y}^{\text{out}})$,

$$\dot{\mathbf{w}} = \mathbb{A}^{(w)} \mathbf{w} + \mathbf{n}^{(w)}, \quad (\text{B19})$$

where

$$\mathbb{A}^{(w)} = \begin{pmatrix} [\mathbb{A}^{(w)}]_{4 \times 4} & 0_{4 \times 2} \\ \sqrt{2\kappa} f^{\text{out}}(t) \mathbb{1}_2 & 0_{2 \times 2} \end{pmatrix}, \quad (\text{B20})$$

with $\mathbb{1}_n$ and $0_{m \times n}$ respectively being an identity matrix and a matrix full of 0s of corresponding dimensions. For the

new 6×6 diffusion matrix, we obtain

$$\mathbb{D}^{(w)} = \begin{pmatrix} [\mathbb{D}^{(v)}]_{4 \times 4} & -f^{\text{out}}(t) \sqrt{2\kappa} \mathbb{1}_2 \\ -f^{\text{out}} \sqrt{2\kappa} \mathbb{1}_2 & [f^{\text{out}}(t)]^2 2\kappa \mathbb{1}_2 \end{pmatrix}. \quad (\text{B21})$$

In these definitions, the covariance matrix $\mathbb{W} = \langle \mathbf{w} \circ \mathbf{w} \rangle$ can be obtained as a solution of the Lyapunov equation

$$\dot{\mathbb{W}} = \mathbb{A}^{(w)} \cdot \mathbb{W} + \mathbb{W} \cdot \mathbb{A}^{(w)} + \mathbb{D}^{(w)} \quad (\text{B22})$$

with the initial condition

$$\mathbb{W}(0) = \text{diag}(1, 1, 2n_0 + 1, 2n_0 + 1, 0, 0). \quad (\text{B23})$$

The equation above shows that the intracavity mode starts at a vacuum state, and the mechanics is initially in a thermal state with mean occupation n_0 .

Removing the first two rows and two columns of \mathbb{W} that correspond to the intracavity mode, we arrive to the relevant covariance matrix that describes correlations between mechanics and the pulse. The Lyapunov equation can be further generalized in a fully similar fashion to describe the subsequent red-detuned readout pulse. To do so, one has to extend the vector \mathbf{w} to have the quadratures of the pulse, and properly generalize the matrices $\mathbb{A}^{(w)}$ and $\mathbb{D}^{(w)}$.

APPENDIX C: FIGURES OF NONCLASSICALITY

The formalism of the Heisenberg-Langevin equations allows expression of the output operators $\mathbf{r} = [\mathbf{X}^{\text{out}}, \mathbf{Y}^{\text{out}}, X_m(\tau), Y_m(\tau)]$ in terms of linear combinations of the input operators. The latter all have Gaussian statistics provided by thermal and vacuum states and, therefore, since the dynamics of the system is described by linear differential equations, the output is in a Gaussian quantum state as well. Owing to this, the output state of our system is completely described by the first two moments of the vector \mathbf{r} : the vector of means $\langle \mathbf{r} \rangle$ and the covariance matrix \mathbb{V} with elements

$$\mathbb{V}_{ij} = \frac{1}{2} \langle \{\mathbf{r}_i - \langle \mathbf{r}_i \rangle, \mathbf{r}_j - \langle \mathbf{r}_j \rangle\} \rangle. \quad (\text{C1})$$

Here $\{\cdot, \cdot\}$ denotes the anticommutator. To evaluate the elements of \mathbb{R} we require the solution for \mathbf{r} that is obtained as a combination of Eqs. (B8) and (B9) and the knowledge of the statistics of the input states. We assume that the intracavity and input optical modes are in vacuum, the mechanical mode is precooled to a thermal state with average occupation n_0 , and the mechanical thermal noise is in a thermal state with average occupation n_{th} .

In this paper we evaluate the nonclassicality of the system using *two-mode squeezing* and *logarithmic negativity* as figures of merit.

The two-mode squeezing is shown by the smallest eigenvalue σ of the covariance matrix of the optomechanical system \mathbb{V} . The two-mode squeezing has an intuitive interpretation as the squeezing that can be extracted from the system by a passive two-mode unitary operation. A convenient way to evaluate the squeezing is to use the units of decibel (dB). The conversion rule reads

$$S_{\text{dB}} = -10 \log_{10} \frac{\sigma}{\sigma_{\text{vac}}}, \quad (\text{C2})$$

where σ is the squeezed eigenvalue. Here σ_{vac} stands for the zero-point fluctuations variance ($\sigma_{\text{vac}} = \langle 0|X^2|0\rangle = 1$ for the choice of units in the present manuscript).

The logarithmic negativity of a bipartite quantum state shows the upper bound of distillable entanglement. It can be computed [11,12] as

$$E_N = \max[0, -\log v_-], \quad (\text{C3})$$

where v_- is the smaller symplectic eigenvalue of the covariance matrix of the partially transposed quantum state. For the state with CM \mathbb{V} written in block form as

$$\mathbb{V} = \begin{bmatrix} \mathbb{V}_L & \mathbb{V}_c \\ \mathbb{V}_c^\top & \mathbb{V}_m \end{bmatrix} \quad (\text{C4})$$

it reads

$$v_- = \frac{1}{\sqrt{2}} \sqrt{\Sigma_V - \sqrt{\Sigma_V^2 - 4 \det \mathbb{V}}} \quad (\text{C5})$$

with $\Sigma_V = \det V_m + \det V_L - 2 \det V_c$.

APPENDIX D: GENERATION OF NONCLASSICAL CORRELATIONS IN THE ADIABATIC REGIME

In this section we investigate the generation of nonclassical correlations in the adiabatic regime. This allows us to obtain order-of-magnitude estimates for the robustness of the protocol used in the main text.

The optomechanical system operates in the adiabatic regime, when the cavity decay rate κ exceeds other characteristic rates of the system (optomechanical coupling g and the heating rate Γ). In this case, the intracavity optical mode almost instantly tracks changes in the system and can be eliminated. Formally, this is can be written by equating the derivatives of intracavity quadratures to zero in Eq. (B4).

The light-matter (LM) covariance matrix of the optomechanical system reads

$$\mathbb{V}_{\text{LM}} = \begin{pmatrix} v_L \mathbb{1}_2 & v_c \mathbb{1}_2 \\ v_c \mathbb{1}_2 & v_M \mathbb{1}_2 \end{pmatrix} + \Gamma \begin{pmatrix} n_L \mathbb{1}_2 & n_C \mathbb{1}_2 \\ n_C \mathbb{1}_2 & n_M \mathbb{1}_2 \end{pmatrix}, \quad (\text{D1})$$

where the first matrix corresponds to the unitary dynamics described by the input-output relations Eq. (1), and

the second matrix contains the influence of the noise from the thermal mechanical bath. The elements of the matrices read (n_0 is the initial occupation of the mechanics)

$$v_L = 2\mathcal{G}(n_0 + 1) - 2n_0 - 1, \quad v_M = 2\mathcal{G}(n_0 + 1) - 1, \quad (\text{D2a})$$

$$v_c = 2\sqrt{\mathcal{G}(\mathcal{G} - 1)}(n_0 + 1), \quad (\text{D2b})$$

and

$$n_M = \frac{\kappa}{g^2}(\mathcal{G} - 1) \approx 2\tau, \quad (\text{D3a})$$

$$n_L = \frac{\kappa(\mathcal{G}^2 - 1) - 4\mathcal{G}g^2\tau}{g^2(\mathcal{G} - 1)} \approx 0, \quad (\text{D3b})$$

$$n_C = \frac{1}{g^2} \sqrt{\frac{\mathcal{G}}{\mathcal{G} - 1}} [\kappa(\mathcal{G} - 1) - 2g^2\tau] \approx \tau \sqrt{\ln \mathcal{G}}. \quad (\text{D3c})$$

The approximate estimates for $n_{M,L,C}$ are obtained by expansion in g/κ up to the linear term and are valid for weak coupling.

From Eqs. (D3) we see that the thermal bath manifests itself in the form of additive noise with variance proportional to $\Gamma\tau$. Therefore, a condition for the thermal noise to not influence the two-mode squeezing is this variance being small enough, $\Gamma\tau \leq 1$.

In what follows we assume that the thermal noise is not present and analyze the unitary input-output relations Eq. (1) to investigate the squeezing detection protocol. The covariance matrix of the optomechanical system is then represented by the first summand in Eq. (D1). The eigenvalues of this matrix can be expressed as

$$\sigma = \xi \cdot \mathbb{V}_{\text{LM}} \cdot \xi, \quad (\text{D4})$$

where

$$\xi = (\cos \theta_1 \cos \phi, \sin \theta_1 \cos \phi, \cos \theta_2 \sin \phi, \sin \theta_2 \sin \phi). \quad (\text{D5})$$

This corresponds to taking the first value from the diagonal of the CM after transformation to the eigenbasis, in correspondence with Eq. (3). The eigenvalue then reads

$$\sigma = \cos^2 \phi v_L + \sin^2 \phi v_M + \cos(\theta_1 - \theta_2) \sin 2\phi v_c. \quad (\text{D6})$$

The first two summands are non-negative, as $v_L > 1$ and $v_M > 1$. Hence, σ' is minimized when $v_c \sin 2\phi < 0$ and

$\theta_1 = \theta_2$. The optimal value of ϕ in this case is defined by

$$\cos \phi = -\frac{\sqrt{2}v_c \sqrt{\frac{\sqrt{4v_c^2 + (v_L - v_M)^2}}{\sqrt{4v_c^2 + (v_L - v_M)^2} + v_L - v_M}}}{\sqrt{4v_c^2 + (v_L - v_M)^2}}. \quad (\text{D7})$$

Practically, it means that in order to detect the two-mode squeezing in such a system, one should detect the same quadratures of both subsystems and superpose them with the weighting factors $\cos \phi$, $\sin \phi$.

Note that the angles $\theta_{1,2}$ (or, rather, the difference $\delta\theta = \theta_1 - \theta_2$) should be defined before the experiment, as they define the homodyne phases. As follows from Eq. (D6), a divergence from the optimal $\delta\theta = 0$ is equivalent to the reduction of correlations between the subsystems that are quantified by the value v_c . In contrast, the angle ϕ can be determined in postprocessing the data. This, however, does not allow us to regain the correlations lost due to erroneous value of $\delta\theta$.

An estimate for the required precision for setting $\delta\theta$ can be obtained by a direct calculation. Substituting Eqs. (D7) and (D2) into Eq. (D6) straightforwardly yields a complicated expression for the eigenvalue as a function of \mathcal{G} , n_0 , and $\delta\theta$. In the limit of high initial occupation $n_0 \gg 1$ and strong coupling $\mathcal{G} \gg 1$, the condition of observation of the two-mode squeezing $\sigma < 1$ reduces to the simple expression

$$\theta^2 < \frac{1}{2\mathcal{G}n_0}. \quad (\text{D8})$$

This shows that a 2 orders of magnitude increase of the initial mechanical occupation requires an order of magnitude higher precision in setting the homodyne angles. The initial mechanical occupation is the major factor that determines the required precision. This is apparently because it is n_0 that determines the spread of the final quantum states that have to be matched to observe the quantum squeezing.

memory in room-temperature atoms, *Commun. Phys.* **1**, 55 (2018).

- [4] Jian-Peng Dou, Ai-Lin Yang, Mu-Yan Du, Di Lao, Hang Li, Xiao-Ling Pang, Jun Gao, Lu-Feng Qiao, Hao Tang, and Xian-Min Jin, Direct observation of broadband nonclassical states in a room-temperature light-matter interface, *npj Quantum Inf.* **4**, 1 (2018).
- [5] Timur Iskhakov, Maria V. Chekhova, and Gerd Leuchs, Generation and Direct Detection of Broadband Mesoscopic Polarization-Squeezed Vacuum, *Phys. Rev. Lett.* **102**, 183602 (2009).
- [6] J. U. Fürst, D. V. Strekalov, D. Elser, A. Aiello, U. L. Andersen, Ch. Marquardt, and G. Leuchs, Quantum Light from a Whispering-Gallery-Mode Disk Resonator, *Phys. Rev. Lett.* **106**, 113901 (2011).
- [7] Martin A. Finger, Timur Sh. Iskhakov, Nicolas Y. Joly, Maria V. Chekhova, and Philip St. J. Russell, Raman-Free, Noble-Gas-Filled Photonic-Crystal Fiber Source for Ultrafast, Very Bright Twin-Beam Squeezed Vacuum, *Phys. Rev. Lett.* **115**, 143602 (2015).
- [8] Xinrui Wei, Jiteng Sheng, Yuelong Wu, Wuming Liu, and Haibin Wu, Twin-beam-enhanced displacement measurement of a membrane in a cavity, arXiv:1902.04288.
- [9] A. I. Lvovsky, in *Photonics* (John Wiley & Sons, Ltd, New Jersey, 2015), p. 121.
- [10] Roman Schnabel, Squeezed states of light and their applications in laser interferometers, *Phys. Rep.* **684**, 1 (2017).
- [11] Julien Laurat, Gaëlle Keller, José Augusto Oliveira-Huguenin, Claude Fabre, Thomas Coudreau, Alessio Serafini, Gerardo Adesso, and Fabrizio Illuminati, Entanglement of two-mode Gaussian states: Characterization and experimental production and manipulation, *J. Opt. B* **7**, S577 (2005).
- [12] Christian Weedbrook, Stefano Pirandola, Raúl García-Patrón, Nicolas J. Cerf, Timothy C. Ralph, Jeffrey H. Shapiro, and Seth Lloyd, Gaussian quantum information, *Rev. Mod. Phys.* **84**, 621 (2012).
- [13] V. Josse, A. Dantan, A. Bramati, M. Pinard, and E. Giacobino, Continuous Variable Entanglement using Cold Atoms, *Phys. Rev. Lett.* **92**, 123601 (2004).
- [14] B. B. Blinov, D. L. Moehring, L.-M. Duan, and C. Monroe, Observation of entanglement between a single trapped atom and a single photon, *Nature* **428**, 153 (2004).
- [15] Jacob F. Sherson, Hanna Krauter, Rasmus K. Olsson, Brian Julsgaard, Clemens Hammerer, Ignacio Cirac, and Eugene S. Polzik, Quantum teleportation between light and matter, *Nature* **443**, 557 (2006).
- [16] T. A. Palomaki, J. D. Teufel, R. W. Simmonds, and K. W. Lehnert, Entangling mechanical motion with microwave fields, *Science* **342**, 710 (2013).
- [17] T. A. Palomaki, J. W. Harlow, J. D. Teufel, R. W. Simmonds, and K. W. Lehnert, Coherent state transfer between itinerant microwave fields and a mechanical oscillator, *Nature* **495**, 210 (2013).
- [18] Sungkun Hong, Ralf Riedinger, Igor Marinković, Andreas Wallucks, Sebastian G. Hofer, Richard A. Norte, Markus Aspelmeyer, and Simon Gröblacher, Hanbury Brown and Twiss interferometry of single phonons from an optomechanical resonator, *Science* **358**, 203 (2017).
- [19] Ralf Riedinger, Andreas Wallucks, Igor Marinković, Clemens Löschner, Markus Aspelmeyer, Sungkun Hong,

- and Simon Gröblacher, Remote quantum entanglement between two micromechanical oscillators, *Nature* **556**, 473 (2018).
- [20] D. Vitali, S. Gigan, A. Ferreira, H. R. Böhm, P. Tombesi, A. Guerreiro, V. Vedral, A. Zeilinger, and M. Aspelmeyer, Optomechanical Entanglement between a Movable Mirror and a Cavity Field, *Phys. Rev. Lett.* **98**, 030405 (2007).
- [21] C. Genes, A. Mari, P. Tombesi, and D. Vitali, Robust entanglement of a micromechanical resonator with output optical fields, *Phys. Rev. A* **78**, 032316 (2008).
- [22] Sebastian G. Hofer, Witold Wieczorek, Markus Aspelmeyer, and Clemens Hammerer, Quantum entanglement and teleportation in pulsed cavity optomechanics, *Phys. Rev. A* **84**, 052327 (2011).
- [23] Andrey A. Rakhubovsky and Radim Filip, Robust entanglement with a thermal mechanical oscillator, *Phys. Rev. A* **91**, 062317 (2015).
- [24] Muddassar Rashid, Tommaso Tufarelli, James Bateman, Jamie Vovrosh, David Hempston, M. S. Kim, and Hendrik Ulbricht, Experimental Realization of a Thermal Squeezed State of Levitated Optomechanics, *Phys. Rev. Lett.* **117**, 273601 (2016).
- [25] Daniel Goldwater, Benjamin Stickler, Lukas Martinetz, Tracy E. Northup, Klaus Hornberger, and James Millen, Levitated electromechanics: All-electrical cooling of charged nano- and micro-particles, *Quantum Sci. Technol.* **4**, 024003 (2018).
- [26] Uroš Delic, Manuel Reisenbauer, David Grass, Nikolai Kiesel, Vladan Vuletic, and Markus Aspelmeyer, Cavity Cooling of a Levitated Nanosphere by Coherent Scattering, *Phys. Rev. Lett.* **122**, 123602 (2019).
- [27] Dominik Windey, Carlos Gonzalez-Ballester, Patrick Maurer, Lukas Novotny, Oriol Romero-Isart, and René Reimann, Cavity-Based 3d Cooling of a Levitated Nanoparticle via Coherent Scattering, *Phys. Rev. Lett.* **122**, 123601 (2019).
- [28] Nadine Meyer, Andrés de los Rios Sommer, Pau Mestres, Jan Gieseler, Vijay Jain, Lukas Novotny, and Romain Quidant, Resolved-Sideband Cooling of a Levitated Nanoparticle in the Presence of Laser Phase Noise, *Phys. Rev. Lett.* **123**, 153601 (2019).
- [29] Uroš Delic, Manuel Reisenbauer, Kahan Dare, David Grass, Vladan Vuletic, Nikolai Kiesel, and Markus Aspelmeyer, Cooling of a levitated nanoparticle to the motional quantum ground state, *Science* **367**, 892 (2020).
- [30] D. E. Chang, C. A. Regal, S. B. Papp, D. J. Wilson, J. Ye, O. Painter, H. J. Kimble, and P. Zoller, Cavity opto-mechanics using an optically levitated nanosphere, *Proc. Natl Acad. Sci.* **107**, 1005 (2010).
- [31] O. Romero-Isart, A. C. Pflanzer, M. L. Juan, R. Quidant, N. Kiesel, M. Aspelmeyer, and J. I. Cirac, Optically levitating dielectrics in the quantum regime: Theory and protocols, *Phys. Rev. A* **83**, 013803 (2011).
- [32] Ondřej Černotík and Radim Filip, Strong mechanical squeezing for a levitated particle by coherent scattering, *Phys. Rev. Res.* **2**, 013052 (2020).
- [33] Henning Rudolph, Klaus Hornberger, and Benjamin A. Stickler, Entangling levitated nanoparticles by coherent scattering, *Phys. Rev. A* **101**, 011804 (2020).
- [34] Lu-Ming Duan, G. Giedke, J. I. Cirac, and P. Zoller, Inseparability Criterion for Continuous Variable Systems, *Phys. Rev. Lett.* **84**, 2722 (2000).
- [35] S. Barzanjeh, E. S. Redchenko, M. Peruzzo, M. Wulf, D. P. Lewis, G. Arnold, and J. M. Fink, Stationary entangled radiation from micromechanical motion, *Nature* **570**, 480 (2019).
- [36] Junxin Chen, Massimiliano Rossi, David Mason, and Albert Schliesser, Entanglement of propagating optical modes via a mechanical interface, *Nat. Commun.* **11**, 1 (2020).
- [37] Francesco Fogliano, Benjamin Besga, Antoine Reigue, Laure Mercier de Lépinay, Philip Heringlake, Clement Gouriou, Eric Eyraud, Wolfgang Wernsdorfer, Benjamin Pigeau, and Olivier Arcizet, Ultrasensitive nano-optomechanical force sensor at dilution temperatures, arXiv:2009.02912.
- [38] Liu Qiu, Itay Shomroni, Paul Seidler, and Tobias J. Kippenberg, Laser Cooling of a Nanomechanical Oscillator to Its Zero-Point Energy, *Phys. Rev. Lett.* **124**, 173601 (2020).
- [39] Xizheng Ma, Jeremie J. Viennot, Shlomi Kotler, John D. Teufel, and Konrad W. Lehnert, Nonclassical energy squeezing of a macroscopic mechanical oscillator, arXiv:2005.04260.
- [40] Ivan Galinskiy, Yeghishe Tsaturyan, Michał Parniak, and Eugene S. Polzik, Phonon counting thermometry of an ultracoherent membrane resonator near its motional ground state, arXiv:2005.14173.
- [41] Lisa Kleybolte, Pascal Gwecke, Andreas Sawadsky, Mikhail Korobko, and Roman Schnabel, Squeezed-light interferometry on a cryogenically-cooled micro-mechanical membrane, arXiv:2008.02560.
- [42] D. Rugar, R. Budakian, H. J. Mamin, and B. W. Chui, Single spin detection by magnetic resonance force microscopy, *Nature* **430**, 329 (2004).
- [43] Andrew A. Geraci, Scott B. Papp, and John Kitching, Short-Range Force Detection Using Optically Cooled Levitated Microspheres, *Phys. Rev. Lett.* **105**, 101101 (2010).
- [44] Asimina Arvanitaki and Andrew A. Geraci, Detecting High-Frequency Gravitational Waves with Optically Levitated Sensors, *Phys. Rev. Lett.* **110**, 071105 (2013).
- [45] Gambhir Ranjit, Mark Cunningham, Kirsten Casey, and Andrew A. Geraci, Zeptoneutron force sensing with nanospheres in an optical lattice, *Phys. Rev. A* **93**, 053801 (2016).
- [46] M. Armano *et al.*, Sub-Femto-g Free Fall for Space-Based Gravitational Wave Observatories: LISA Pathfinder Results, *Phys. Rev. Lett.* **116**, 231101 (2016).
- [47] David Hempston, Jamie Vovrosh, Marko Toros, George Winstone, Muddassar Rashid, and Hendrik Ulbricht, Force sensing with an optically levitated charged nanoparticle, *Appl. Phys. Lett.* **111**, 133111 (2017).
- [48] Erik Hebestreit, Martin Frimmer, René Reimann, Christoph Dellago, Francesco Ricci, and Lukas Novotny, Calibration and temperature measurement of levitated optomechanical sensors, *Rev. Sci. Instrum.* **89**, 033111 (2018).
- [49] Zhujing Xu and Tongcang Li, Detecting Casimir torque with an optically levitated nanorod, *Phys. Rev. A* **96**, 033843 (2017).

- [50] Erik Hebestreit, Martin Frimmer, René Reimann, and Lukas Novotny, Sensing Static Forces with Free-Falling Nanoparticles, *Phys. Rev. Lett.* **121**, 063602 (2018).
- [51] Fernando Monteiro, Sumita Ghosh, Adam Getzels Fine, and David C. Moore, Optical levitation of 10- μg spheres with nano- g acceleration sensitivity, *Phys. Rev. A* **96**, 063841 (2017).
- [52] George Winstone, Robert Bennett, Markus Rademacher, Muddassar Rashid, Stefan Buhmann, and Hendrik Ulbricht, Direct measurement of the electrostatic image force of a levitated charged nanoparticle close to a surface, *Phys. Rev. A* **98**, 053831 (2018).
- [53] F. Ricci, M. T. Cuairan, G. P. Conangla, A. W. Schell, and R. Quidant, Accurate mass measurement of a levitated nanomechanical resonator for precision force-sensing, *Nano Lett.* **19**, 6711 (2019).
- [54] Massimiliano Rossi, David Mason, Junxin Chen, and Albert Schliesser, Observing and Verifying the Quantum Trajectory of a Mechanical Resonator, *Phys. Rev. Lett.* **123**, 163601 (2019).
- [55] Itay Shomroni, Liu Qiu, Daniel Malz, Andreas Nunnenkamp, and Tobias J. Kippenberg, Optical backaction-evasive measurement of a mechanical oscillator, *Nat. Commun.* **10**, 2086 (2019).
- [56] Sh. Barzanjeh, D. Vitali, P. Tombesi, and G. J. Milburn, Entangling optical and microwave cavity modes by means of a nanomechanical resonator, *Phys. Rev. A* **84**, 042342 (2011).
- [57] T. Bagci, A. Simonsen, S. Schmid, L. G. Villanueva, E. Zeuthen, J. Appel, J. M. Taylor, A. Sørensen, K. Usami, A. Schliesser, and E. S. Polzik, Optical detection of radio waves through a nanomechanical transducer, *Nature* **507**, 81 (2014).
- [58] Oriol Romero-Isart, Quantum superposition of massive objects and collapse models, *Phys. Rev. A* **84**, 052121 (2011).
- [59] William Marshall, Christoph Simon, Roger Penrose, and Dik Bouwmeester, Towards Quantum Superpositions of a Mirror, *Phys. Rev. Lett.* **91**, 130401 (2003).
- [60] A. Vinante, R. Mezzena, P. Falferi, M. Carlesso, and A. Bassi, Improved Noninterferometric Test of Collapse Models Using Ultracold Cantilevers, *Phys. Rev. Lett.* **119**, 110401 (2017).
- [61] A. Vinante, A. Pontin, M. Rashid, M. Toroš, P. F. Barker, and H. Ulbricht, Testing collapse models with levitated nanoparticles: Detection challenge, *Phys. Rev. A* **100**, 012119 (2019).
- [62] James Millen and Jan Gieseler, in *Thermodynamics in the Quantum Regime: Fundamental Aspects and New Directions*, edited by Felix Binder, Luis A. Correa, Christian Gogolin, Janet Anders, and Gerardo Adesso, Fundamental Theories of Physics (Springer International Publishing, Cham, 2018), p. 853.
- [63] Gonzalo Manzano, Fernando Galve, Roberta Zambrini, and Juan M. R. Parrondo, Entropy production and thermodynamic power of the squeezed thermal reservoir, *Phys. Rev. E* **93**, 052120 (2016).
- [64] Wolfgang Niedenzu, David Gelbwaser-Klimovsky, Abraham G. Kofman, and Gershon Kurizki, On the operation of machines powered by quantum non-thermal baths, *New J. Phys.* **18**, 083012 (2016).
- [65] Jan Klaers, Stefan Faelt, Atac Imamoglu, and Emre Togan, Squeezed Thermal Reservoirs as a Resource for a Nanomechanical Engine beyond the Carnot Limit, *Phys. Rev. X* **7**, 031044 (2017).
- [66] Gonzalo Manzano, Squeezed thermal reservoir as a generalized equilibrium reservoir, *Phys. Rev. E* **98**, 042123 (2018).
- [67] G. Manzano, Entropy production and fluctuations in a Maxwell's refrigerator with squeezing, *Eur. Phys. J. Spec. Top.* **227**, 285 (2018).
- [68] Jan Klaers, Landauer's Erasure Principle in a Squeezed Thermal Memory, *Phys. Rev. Lett.* **122**, 040602 (2019).
- [69] James Millen and André Xuereb, Perspective on quantum thermodynamics, *New J. Phys.* **18**, 011002 (2016).
- [70] A. Tomadin, S. Diehl, M. D. Lukin, P. Rabl, and P. Zoller, Reservoir engineering and dynamical phase transitions in optomechanical arrays, *Phys. Rev. A* **86**, 033821 (2012).
- [71] Uzma Akram, William Munro, Kae Nemoto, and G. J. Milburn, Photon-phonon entanglement in coupled optomechanical arrays, *Phys. Rev. A* **86**, 042306 (2012).
- [72] Lu Qi, Yan Xing, Hong-Fu Wang, Ai-Dong Zhu, and Shou Zhang, Simulating Z_2 topological insulators via a one-dimensional cavity optomechanical cells array, *Opt. Express* **25**, 17948 (2017).
- [73] Radim Filip and Vojtěch Kupčík, Robust Gaussian entanglement with a macroscopic oscillator at thermal equilibrium, *Phys. Rev. A* **87**, 062323 (2013).
- [74] R. W. Andrews, R. W. Peterson, T. P. Purdy, K. Cicak, R. W. Simmonds, C. A. Regal, and K. W. Lehnert, Bidirectional and efficient conversion between microwave and optical light, *Nat. Phys.* **10**, 321 (2014).
- [75] A. P. Higginbotham, P. S. Burns, M. D. Urmey, R. W. Peterson, N. S. Kampel, B. M. Brubaker, G. Smith, K. W. Lehnert, and C. A. Regal, Electro-optic correlations improve an efficient mechanical converter, *Nat. Phys.* **14**, 1038 (2018).
- [76] Nikita Vostrosablin, Andrey A. Rakhubovsky, and Radim Filip, Pulsed quantum continuous-variable optoelectromechanical transducer, *Opt. Express* **25**, 18974 (2017).
- [77] Nikita Vostrosablin, Andrey A. Rakhubovsky, Ulrich B. Hoff, Ulrik L. Andersen, and Radim Filip, Quantum optomechanical transducer with ultrashort pulses, *New J. Phys.* **20**, 083042 (2018).
- [78] Uros Delic, David Grass, Manuel Reisenbauer, Tobias Damm, Martin Weitz, Nikolai Kiesel, and Markus Aspelmeyer, Levitated cavity optomechanics in high vacuum, *Quantum Sci. Technol.* **5**, 025006 (2020).
- [79] Oriol Romero-Isart, Mathieu L. Juan, Romain Quidant, and J. Ignacio Cirac, Toward quantum superposition of living organisms, *New J. Phys.* **12**, 033015 (2010).
- [80] Justin D. Cohen, Séan M. Meenehan, and Oskar Painter, Optical coupling to nanoscale optomechanical cavities for near quantum-limited motion transduction, *Opt. Express* **21**, 11227 (2013).
- [81] Vijay Jain, Jan Gieseler, Clemens Moritz, Christoph Dellago, Romain Quidant, and Lukas Novotny, Direct Measurement of Photon Recoil from a Levitated Nanoparticle, *Phys. Rev. Lett.* **116**, 243601 (2016).

- [82] Radim Filip and Andrey A. Rakhubovsky, Transfer of non-Gaussian quantum states of mechanical oscillator to light, *Phys. Rev. A* **92**, 053804 (2015).
- [83] Andrey A. Rakhubovsky and Radim Filip, Photon-phonon-photon transfer in optomechanics, *Sci. Rep.* **7**, 46764 (2017).
- [84] Henning Vahlbruch, Moritz Mehmet, Karsten Danzmann, and Roman Schnabel, Detection of 15 dB Squeezed States of Light and Their Application for the Absolute Calibration of Photoelectric Quantum Efficiency, *Phys. Rev. Lett.* **117**, 110801 (2016).
- [85] Martin Šiler, Luca Ornigotti, Oto Brzobohatý, Petr Jákl, Artem Ryabov, Viktor Holubec, Pavel Zemánek, and Radim Filip, Diffusing up the Hill: Dynamics and Equipartition in Highly Unstable Systems, *Phys. Rev. Lett.* **121**, 230601 (2018).
- [86] C. K. Law, Interaction between a moving mirror and radiation pressure: A Hamiltonian formulation, *Phys. Rev. A* **51**, 2537 (1995).
- [87] Markus Aspelmeyer, Tobias J. Kippenberg, and Florian Marquardt, Cavity optomechanics, *Rev. Mod. Phys.* **86**, 1391 (2014).
- [88] Warwick P. Bowen and Gerard J. Milburn, *Quantum Optomechanics* (CRC Press, Boca Raton, 2015).
- [89] Olivier Morin, Claude Fabre, and Julien Laurat, Experimentally Accessing the Optimal Temporal Mode of Traveling Quantum Light States, *Phys. Rev. Lett.* **111**, 213602 (2013).
- [90] B. Brecht, Dileep V. Reddy, C. Silberhorn, and M. G. Raymer, Photon Temporal Modes: A Complete Framework for Quantum Information Science, *Phys. Rev. X* **5**, 041017 (2015).